

2017


Effects of Gait Speed of Femoroacetabular Joint Forces

Joshua T. Weinhandl

Bobbie S. Irmisher
Old Dominion University

Zachary A. Sievert
Old Dominion University, zsiev001@odu.edu

Follow this and additional works at: https://digitalcommons.odu.edu/hms_fac_pubs

 Part of the [Movement and Mind-Body Therapies Commons](#), and the [Musculoskeletal System Commons](#)

Repository Citation

Weinhandl, Joshua T.; Irmisher, Bobbie S.; and Sievert, Zachary A., "Effects of Gait Speed of Femoroacetabular Joint Forces" (2017). *Human Movement Sciences Faculty Publications*. 15.
https://digitalcommons.odu.edu/hms_fac_pubs/15

Original Publication Citation

Weinhandl, J. T., Irmischer, B. S., & Sievert, Z. A. (2017). Effects of gait speed of femoroacetabular joint forces. *Applied Bionics and Biomechanics*, 1-7. doi: 10.1155/2017/6432969

Research Article

Effects of Gait Speed of Femoroacetabular Joint Forces

Joshua T. Weinhandl,¹ Bobbie S. Irmischer,² and Zachary A. Sievert²

¹Department of Kinesiology, Recreation, and Sports Studies, The University of Tennessee, Knoxville, TN, USA

²Department of Human Movement Sciences, Old Dominion University, Norfolk, VA, USA

Correspondence should be addressed to Joshua T. Weinhandl; jweinhan@utk.edu

Received 8 August 2016; Revised 30 November 2016; Accepted 4 January 2017; Published 2 February 2017

Academic Editor: Simo Saarakkala

Copyright © 2017 Joshua T. Weinhandl et al. This is an open access article distributed under the Creative Commons Attribution License, which permits unrestricted use, distribution, and reproduction in any medium, provided the original work is properly cited.

Alterations in hip joint loading have been associated with diseases such as arthritis and osteoporosis. Understanding the relationship between gait speed and hip joint loading in healthy hips may illuminate changes in gait mechanics as walking speed deviates from preferred. The purpose of this study was to quantify hip joint loading during the gait cycle and identify differences with varying speed using musculoskeletal modeling. Ten, healthy, physically active individuals performed walking trials at their preferred speed, 10% faster, and 10% slower. Kinematic, kinetic, and electromyographic data were collected and used to estimate hip joint force via a musculoskeletal model. Vertical ground reaction forces, hip joint force planar components, and the resultant hip joint force were compared between speeds. There were significant increases in vertical ground reaction forces and hip joint forces as walking speed increased. Furthermore, the musculoskeletal modeling approach employed yielded hip joint forces that were comparable to previous simulation studies and in vivo measurements and was able to detect changes in hip loading due to small deviations in gait speed. Applying this approach to pathological and aging populations could identify specific areas within the gait cycle where force discrepancies may occur which could help focus management of care.

1. Introduction

During gait, hip joint loading is important in maintaining healthy bone structure. The relationship between inadequate lower extremity loading and poor bone density, particularly in aging females, is well established [1]. However, excessive hip joint loading may increase the likelihood of developing osteoarthritis in healthy hips [2]. Hip joint forces and stresses have been studied using in vivo (e.g., implanted sensors) and in silico (e.g., laboratory based motion capture) approaches. In vitro studies have consistently measured hip joint forces higher than those estimated in vivo [3, 4]. Unfortunately, it is difficult to directly compare findings between study types in healthy populations due to limited subject numbers and invasive techniques necessary for direct measurement methodologies. The less invasive nature of analytical modeling allows for force estimation with reduced subject risk and financial cost. However, musculoskeletal models face their own limitations [5].

A model estimating hip joint forces throughout the gait cycle in healthy hips is needed to provide a reference for

comparison to pathological or at-risk populations. Lower extremity kinematics and kinetics in gait have been extensively studied. Increasing walking speed has been associated with increased ground reaction forces during toe off and heel contact stages [6] and higher peak resultant forces at the hip [3]. Examining the relationship between speed and hip joint loading in healthy hips may illuminate changes in gait mechanics as walking speed deviates from preferred.

Recently, musculoskeletal models have been used to predict hip joint loading at different gait speeds [7, 8]. While these studies reported hip contact forces comparable to those measured in vivo [3], they employed static optimization to estimate muscle forces. Static optimization is an inverse dynamics-based method that partitions the net joint moment amongst individual muscles by minimizing a given performance criterion (e.g., sum of squared muscle activations). This makes static optimization highly dependent on accurate kinematic data collection. Even so, the measured kinematics are dynamically inconsistent with the measured ground reaction forces, yielding a set of residual

forces and moments acting on the model center of mass that have no physical meaning. Furthermore, the time-independent nature of static optimization makes it difficult to incorporate muscle physiology and can inhibit the ability to predict co-contraction of antagonistic muscles. On the other hand, Residual Reduction Algorithm (RRA) [9] and Computed Muscle Control (CMC) [10] can be utilized to produce a dynamically consistent model. RRA uses the inverse dynamics result and reduces the magnitude of the residuals by slightly adjusting the joint kinematics and model mass properties. CMC is a forward dynamics-based approach that utilizes feedback control theory to predict a set of muscle excitations that will produce kinematics that closely match the measured kinematics while including muscle physiology and activation dynamics. Furthermore, Giarmatzis et al. [7] employed rather large speed increments (1 km/hr intervals) and it remains unknown how hip joint loading is affected by small deviations from preferred walking speed. Therefore, the purpose of this paper was to identify differences in hip joint loading as walking speed varies from preferred by $\pm 10\%$. It was hypothesized that hip joint forces would increase as walking speed increased.

2. Methods

2.1. Subjects. Ten healthy individuals volunteered to participate in the study (age: 25.8 ± 6.2 yr; height: 1.75 ± 0.09 m; and mass: 77.3 ± 10.8 kg). Inclusion criterion required participants be between 18 and 35 years of age and physically active. Physically active was defined as performing at least 30 minutes of exercise three times a week. An injury to the lower extremities within the past six months and any history of lower extremity surgery were considered exclusionary factors. Prior to data collection, participants were informed of study procedures and provided written informed consent in accordance with institutional guidelines.

2.2. Data Collection. Testing was performed in the Neuromechanics Lab (ODU, Norfolk, VA, USA) using lab standard tennis shoes (Air Max Glide, Nike, Beaverton, OR, USA). Muscle activations were measured at 2000 Hz using a Trigno wireless surface electrode electromagnetic (EMG) system (Delsys Inc., Boston, MA, USA). Three-dimensional marker coordinate data were collected at 200 Hz using an eight-camera motion analysis system (Vicon, Centennial, CO, USA). Ground reaction forces (GRF) were measured at 1000 Hz with three flush mounted force plates (Bertec, Columbus, OH, USA) in a 10 m walkway. Muscle activations, marker coordinates, and GRF data were collected synchronously. Walking speed was measured with Brower timing gates (Brower Timing Systems, Draper, UT, USA) positioned before the first plate and after the third plate, 2 m apart. Gait speeds were subsequently verified during postprocessing using the force plate data.

Participants completed five walking trials each at their preferred walking speed, 10% faster, and 10% slower. Trials were collected in blocks with all trials of one speed being collected before proceeding to the next speed. Preferred speed

conditions were collected first. Orders for the 10% faster and slower conditions were randomly assigned. Distance between force plates was modified as needed between conditions to accommodate variations in step length due to the altered speeds. Participants performed practice trials before each condition. A trial was considered good if the participant struck the first force plate with the left foot and hit the following two plates with successive right and left footfalls. Trials where the participant did not cleanly hit one of the force plates, targeted the force plates, or were outside of the prescribed speed ($\pm 2.5\%$) were discarded and recollected. For study purposes, the gait cycle was defined from right heel strike on the second force plate to successive right heel strike after the third force plate. Initial right heel strike was defined as the first time point when vertical ground reaction forces on the middle force plate were greater than 10 N. The successive right heel strike was defined as the time point with maximum contralateral hip flexion [11]. Data were time normalized to 100% of the gait cycle for comparison at each percent of motion from successive heel strikes.

EMG surface electrodes were placed on the gluteus medius, tensor fascia latae, rectus femoris, vastus medialis, biceps femoris, semimembranosus, tibialis anterior, and gastrocnemius medialis of the right limb. Muscles of interest were palpated and the skin prepared by gently wiping with an alcohol wipe and shaving as necessary. Wireless EMG electrodes were placed over specific muscles according to guidelines proposed by Rainoldi et al. [12]. Maximum voluntary isometric contractions (MVICs) were collected for each muscle.

Single reflective markers were placed on the skin over specific anatomical landmarks with adhesive tape for calibration purposes only. Calibration markers were placed bilaterally on the acromioclavicular joints, iliac crests, greater trochanters, medial and lateral knee epicondyles, medial and lateral malleoli, first metatarsal heads, and fifth metatarsal heads. Marker tracking in movement trials utilized eight cluster plates positioned on the upper torso and pelvis, as well as bilateral thighs, shanks, and feet. For these tracking clusters, four retroreflective markers were attached to semirigid, molded Orthoplast (Johnson & Johnson, Raynham, MA, USA). Thigh and shank clusters were secured using prewrap and McDavid groin wraps (McDavid, Woodridge, IL, USA). Foot clusters were affixed to lab shoes using industrial strength Velcro. Pelvis and trunk clusters were secured with custom neoprene straps.

Prior to data collection, motion capture system was calibrated according to manufacturer's specifications and force plates were zeroed. When all markers and electrodes were placed on the participant, a three-second static trial was collected. For this trial, the subject was asked to stand motionless with arms crossed high over the chest and each foot on a separate force plate. Calibration markers were removed and technical markers remained.

2.3. Data Analysis. A kinematic model comprised of eight skeletal segments (trunk, pelvis, and bilateral thighs, shanks, and feet) was created from the standing calibration trial [13]

with Visual3D (v4.95, C-Motion Inc., Rockville, MD). Gaps in marker trajectories less than 10 frames were pattern filled using a marker collocated on the same cluster. Raw three-dimensional marker coordinate and GRF data were low-pass filtered using a fourth-order, zero-lag, recursive Butterworth filter with cutoff frequencies of 6 Hz and 50 Hz, respectively. Hip joint centers were placed at 25% of the distance from ipsilateral to contralateral greater trochanter marker [14]. Knee joint centers were the midpoint between femoral epicondyle markers [15] and ankle joint centers were the midpoint between malleoli markers [16]. Segment coordinates systems were defined to describe segment position and orientation using an unweighted least squares procedure [17]. An inverse kinematics algorithm was used to solve for the joint angles that minimized soft tissue artifact and measurement error in the experimentally measured marker positions [18].

EMG data was preamplified and high-pass filtered using fourth-order, zero-lag, recursive Butterworth filter with a cutoff frequency of 10 Hz to remove movement artifact. The signal was full-wave rectified and low-pass filtered with a cutoff frequency of 5 Hz to create a linear envelope. The filtered EMG signals for each muscle were normalized using peak MVIC values.

OpenSim (v3.1, <http://simtk.org>) was used to simulate one gait cycle, from right heel contact to successive right heel contact [9]. An 8-segment, 19-degrees of freedom (dof), musculoskeletal model, modified from the Gait2392 musculoskeletal model provided by OpenSim [19, 20], was scaled for each subject using individual anthropometric data from the calibration trial. Pelvic translation and rotations were modeled with 6-dof. Lumbar and hip motions were modeled as 3-dof ball and socket joints. Knee motions were modeled as a custom 1-dof joint with tibiofemoral translations constrained as a function of knee flexion [21]. Ankle motions were modeled as 1-dof revolute joints. Ninety-two Hill-type contractile elements in series with tendon were used to actuate the model; 43 for each leg and 6 for the torso [22]. Reserve actuators were included for each degree of freedom in the model to provide extra torque if the muscles could not generate the measured accelerations.

Residual forces and moments were minimized using RRA to improve dynamic consistency between measured and modeled ground reaction forces and kinematics [9]. Model kinematics and mass properties were adjusted as indicated, while residual forces and moments were applied to the pelvis. To produce a simulation which closely tracked the experimental data with limited residuals, an outer level optimization algorithm was used to determine RRA input parameters [23]. Muscle forces were estimated using CMC which determines the set of muscle excitations that produce the forces that generate measured accelerations for all degrees of freedom taking into account muscle activation dynamics and force-length-velocity properties [10]. Hip joint forces were calculated using the joint reaction analysis algorithm in OpenSim. Joint reaction analysis calculation details have been previously described by Steele et al. [24]. Simulation was deemed successful if residual forces and torques, as well as reserve actuators, were minimized according to the guidelines specified by Hicks et al. [25], model pelvis and right leg

kinematics were within 2 cm and 2° of measured pelvis and right leg kinematics, and simulated muscle activations were visually similar to participants' recorded EMG.

2.4. Statistical Analysis. Discrete variables were identified from each trial for analysis, including first and second peak vertical GRF, first and second peak vertical HJF, peak posterior HJF, peak lateral HJF, and first and second peak resultant HJF. Differences between speeds for GRF and HJF variables were assessed via separate repeated measures ANOVAs ($p < 0.05$). Due to the exploratory nature of the study, Tukey's LSD post hoc analyses were conducted. Statistical analyses were performed using custom MATLAB code (MathWorks, Natick, MA, USA) and SPSS (SPSS Inc., Chicago, IL, USA).

3. Results

Five men (age: 27.2 ± 6.5 yr; height: 1.83 ± 0.04 m; and mass: 83.5 ± 9.4 kg) and five women (age: 24.4 ± 6.2 yr; height: 1.67 ± 0.04 m; and mass: 71.1 ± 8.7 kg) completed the study. Average gait speed for all participants was 1.34 ± 0.07 m·s⁻¹ for normal trials, 1.21 ± 0.09 m·s⁻¹ for slow trials, and 1.48 ± 0.08 m·s⁻¹ for fast trials.

3.1. Musculoskeletal Model. All simulations closely tracked measured kinematic and kinetic data with *rms* positional errors less than 1.5 cm for pelvic translations, 0.2° for pelvic rotations, and 0.6° for right leg angles (Table 1). The *rms* magnitude of residual forces and torques incurred during these simulations remained less than 6.05 N and 26.26 Nm, respectively, and the *rms* magnitude of reserve actuators was less than 0.1 Nm for all degrees of freedom. Muscle activity employed during simulations demonstrated similar behavior to EMG activity measured during trials. Ensemble curves for measured EMG and CMC derived muscle activations are provided in Figure 1. EMG data for one subject was corrupted during analysis and could not be included.

3.2. Ground Reaction Forces. There was a significant effect of speed for the first peak vertical GRF ($p = 0.007$) but not for the second peak vertical GRF ($p = 0.272$). Post hoc, pairwise comparisons revealed that first peak vertical GRF was significantly lower during slower walking trials (1.08 ± 0.04) than both normal speed (1.11 ± 0.05 ; $p = 0.010$) and faster (1.12 ± 0.05 ; $p = 0.022$) walking trials (Table 2).

3.3. Hip Contact Forces. Peak posterior HJF ($p = 0.013$), second peak vertical HJF ($p = 0.004$), and second peak resultant HJF ($p = 0.004$) were significantly different between speeds (Table 2) (Figure 2). For peak posterior HJF, post hoc analyses indicated that slow walking trials (-2.12 ± 0.56) were significantly lower than normal speed (-2.31 ± 0.63 ; $p = 0.017$) and fast (-2.37 ± 0.68 ; $p = 0.020$) walking trials (Figure 3). Likewise, second peak vertical HJF was significantly greater during fast walking trials (-4.12 ± 0.85) compared to both normal speed (-3.85 ± 0.69 ; $p = 0.037$) and slow (-3.73 ± 0.76 ; $p = 0.012$) walking trials. Lastly, post hoc paired comparisons showed that 2nd peak resultant HJF

TABLE 1: Mean \pm SD *rms* residual forces and moments and *rms* positional error of modeled kinematics for each condition.

	Normal	Faster	Slower
Residual forces (N)			
Fx	2.18 ± 1.22	2.49 ± 1.47	1.97 ± 1.15
Fy	5.99 ± 1.78	5.47 ± 1.97	6.05 ± 1.78
Fz	1.36 ± 0.86	1.43 ± 0.86	1.62 ± 0.78
Residual moments (Nm)			
Mx	18.18 ± 7.13	19.85 ± 6.21	21.10 ± 7.93
My	10.36 ± 4.73	10.55 ± 3.16	9.53 ± 3.93
Mz	22.40 ± 4.75	26.26 ± 5.36	22.38 ± 3.70
Pelvic translations (mm)			
Tx	7.59 ± 2.59	8.89 ± 3.15	8.23 ± 4.64
Ty	14.75 ± 3.38	13.28 ± 4.88	14.40 ± 3.57
Tz	4.20 ± 2.67	4.24 ± 1.89	4.44 ± 2.44
Pelvic rotations (deg.)			
Tilt	0.11 ± 0.06	0.11 ± 0.09	0.13 ± 0.09
List	0.19 ± 0.22	0.14 ± 0.21	0.15 ± 0.21
Rotation	0.02 ± 0.01	0.02 ± 0.01	0.02 ± 0.01
Right hip (deg.)			
Flexion	0.47 ± 0.50	0.59 ± 0.54	0.39 ± 0.41
Adduction	0.10 ± 0.10	0.09 ± 0.07	0.11 ± 0.11
Rotation	0.03 ± 0.05	0.01 ± 0.01	0.01 ± 0.01
Right knee (deg.)			
Flexion	0.15 ± 0.31	0.17 ± 0.41	0.11 ± 0.22
Right ankle (deg.)			
Dorsiflexion	0.05 ± 0.05	0.05 ± 0.04	0.03 ± 0.03

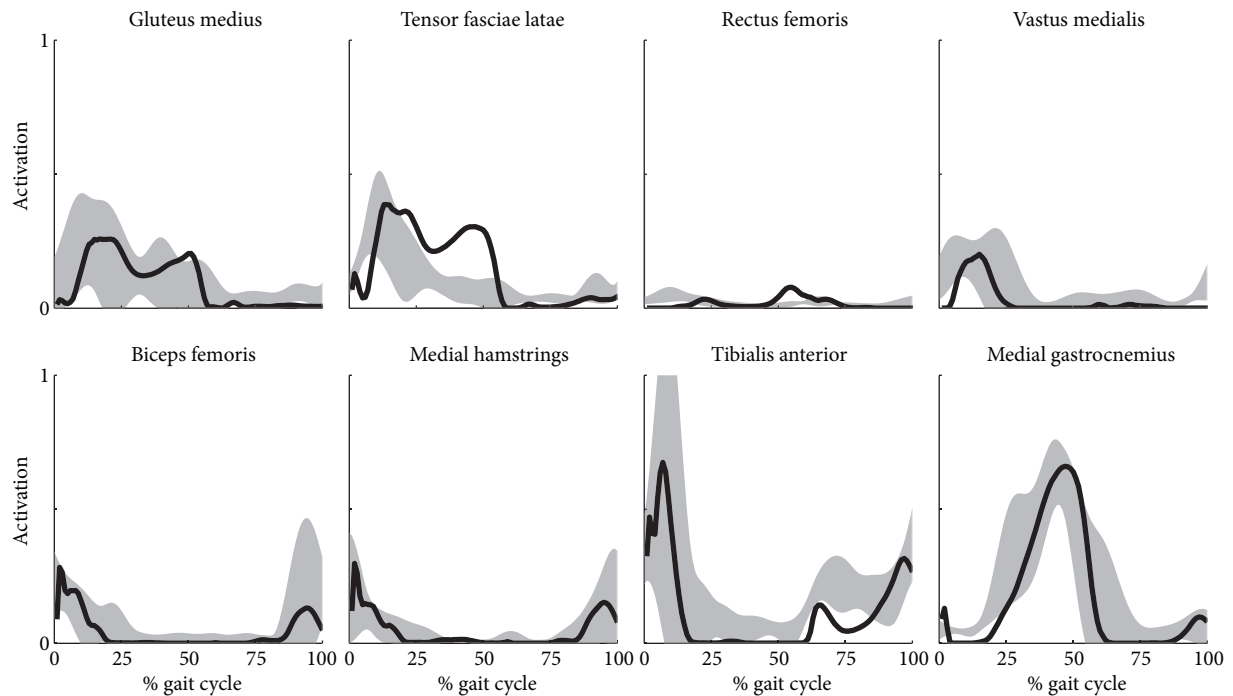


FIGURE 1: Ensemble simulated muscle activations from computed muscle control (solid line) and experimentally measured EMG (shaded area) during normal conditions. Shaded regions represent ± 1 standard deviation of the mean EMG for nine subjects. EMG data were normalized to the muscle specific maximum-recorded signal during MVIC testing. Activations are represented on a spectrum of 0 (fully deactivated) to 1 (fully activated).

TABLE 2: Group means \pm SD for discrete ground reaction forces (GRF) and hip joint reaction forces (HJF). All force variables are presented in bodyweights (BW).

	Normal	Faster	Slower
1st peak vertical GRF ^{bc}	1.11 \pm 0.05	1.12 \pm 0.05	1.08 \pm 0.04
2nd peak vertical GRF	1.11 \pm 0.04	1.12 \pm 0.04	1.10 \pm 0.03
1st peak vertical HJF	-3.25 \pm 0.45	-3.28 \pm 0.50	-3.12 \pm 0.43
2nd peak vertical HJF ^{ac}	-3.85 \pm 0.69	-4.12 \pm 0.85	-3.73 \pm 0.76
Peak posterior HJF ^{bc}	-2.31 \pm 0.63	-2.37 \pm 0.68	-2.12 \pm 0.56
Peak lateral HJF	0.94 \pm 0.18	0.98 \pm 0.25	0.93 \pm 0.18
1st peak resultant HJF	3.39 \pm 0.45	3.42 \pm 0.55	3.26 \pm 0.40
2nd peak resultant HJF ^c	4.61 \pm 0.55	4.88 \pm 0.77	4.41 \pm 0.56

a: significant differences between normal and fast speeds $\pm p < 0.05$.
 b: Significant differences between normal and slow speeds $\pm p < 0.05$.
 c: Significant differences between fast and slow speeds $\pm p < 0.05$.

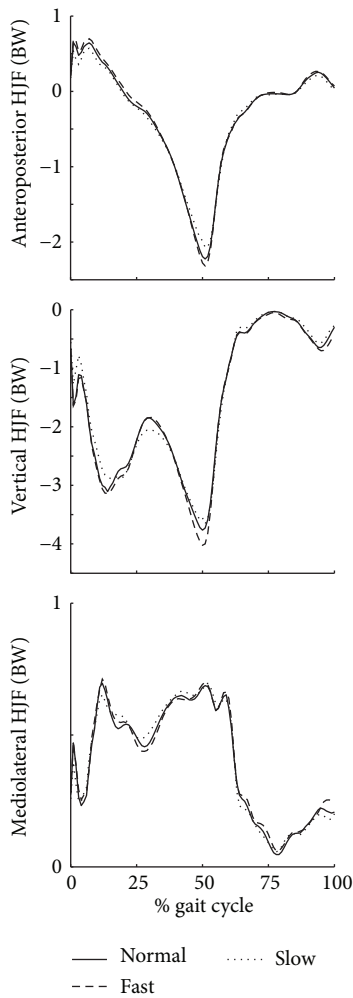


FIGURE 2: Mean ensemble curves of the anteroposterior, vertical, and mediolateral hip joint force (HJF) during the gait cycle. Solid line represents the normal walking condition, dashed line represents the fast walking condition, and dotted line represents the slow walking condition.

(Figure 3) was significantly greater during fast walking trials (4.88 ± 0.77) compared to slow walking trials (4.41 ± 0.56 ; $p = 0.09$). While nonsignificant post hoc analyses also indicated that second peak resultant HJF during normal speed walking

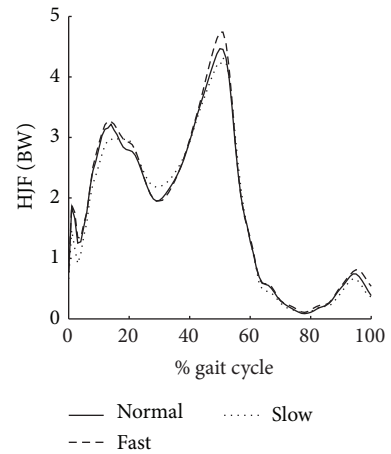


FIGURE 3: Mean ensemble curves of the resultant hip joint force (HJF) during the gait cycle. Solid line represents the normal walking condition, dashed line represents the fast walking condition, and dotted line represents the slow walking condition.

trials (4.61 ± 0.55) trended towards being significantly lower than fast walking trial ($p = 0.060$) and significantly greater than slow walking trials ($p = 0.058$).

4. Discussion

The purpose of this paper was to determine if small changes in gait speed affected hip joint loading throughout the gait cycle. There were significant increases in first peak vertical GRF and peak posterior HJF for fast and normal speed walking conditions compared to slow walking. There were also significant increases in second peak vertical HJF for the fast walking condition compared to both normal speed and slow walking conditions. Finally, second peak resultant HJF was significantly larger in fast walking compared to slow walking and displayed a trend towards significant increase for fast walking compared to normal speed and for normal speed compared to slow walking. These findings partially support our hypothesis that hip joint force would increase as speed increased.

Significant increases of peak force values suggest that there are changes in gait mechanics when participants walk slower and faster than preferred. Peak vertical ground reaction force increased significantly from 1.08 to 1.12 BW from slow to fast conditions. Chung and Wang [6] also observed peak vertical ground forces increased from 0.98 to 1.07 BW during the heel strike stage as speed increased from 80% to 120% of preferred walking speed.

Second peak vertical HJF increased from 3.73 to 4.12 BW between slow and fast speeds, while second peak resultant HJF increased from 4.41 to 4.61 and 4.88 BW between slow, normal, and fast speeds, respectively. Vertical hip joint forces previously reported vary greatly based on study methodology and subject population. The range of vertical hip joint forces reported here is similar to that reported by Crowninshield et al. [26] of 3.3 to 5.0 BW and Röhrle et al. [27] of 2.9 to 6.9 BW. In a similar study, Giarmatzis et al. [7] reported first and second peak resultant HJFs ranged from 4.22 to 5.41 BW and 4.37 to 5.74 BW, respectively, as walking speed increased from 3 to 6 km·hr⁻¹. These values are considerably higher than those reported in the current study, which may be due to methodological differences in estimating muscle forces between Giarmatzis et al. [7] and the current study. Furthermore, Giarmatzis et al. [7] appended reserve actuators to the joints of the model, like the current study, which should be kept smaller than 5% of the respective net joint moment [25]. However, Giarmatzis et al. [7] reported large hip abduction reserve actuator torque which they distributed to the gluteus medius as additional muscle force production which likely increased their HJF estimates.

While the HJFs in the current study are comparable to those reported in other musculoskeletal modeling studies with healthy participants [26, 27], they are higher than those reported in direct measurement methodologies [3] and those estimated using samples with older participants and pathological hips [4, 8]. Bergmann et al. [3] reported peak resultant HJFs of 2.42 BW for slow walking, 2.38 BW for normal walking, and 2.50 BW for fast walking which are 2 BW lower than those found in the current study. Older adults have been suggested to select gait patterns which minimize GRFs and hip stress [28]. Further, reductions in peak GRF have also been associated with pathological hips [29]. Inclusion criteria for the current study required participants to be between the ages of 18 and 35, recreationally active, and healthy. Minimization of hip joint forces may not be a factor in the selection of gait patterns for this population, resulting in higher vertical and resultant hip joint forces.

Even though musculoskeletal models are a valuable tool to investigate skeletal loads during gait, current techniques, including the one adopted here, present several limitations. First, the joints, especially the knee and ankle, are simple models and may limit ability to accurately reproduce subject movement. Second, several parameters defining the muscle functions such as maximum isometric force, tendon slack length, and optimal fiber length cannot be truly subject-specific but rely on published values measured on a limited sample of cadaveric specimens. Third, skeletal geometry such as femoral anteversion and neck length have strong

influences on predicted HJFs [30, 31]. Since we did not have radiographs or computerized tomography scans or our participants we were unable to account for potential between subject variations in femoral anteversion, neck angle, or neck length which may influence our estimates of HJFs. Finally, CMC was utilized to estimate muscle activations, which uses the combination of a static optimization criterion [32] and proportional-derivative control to generate a forward dynamic simulation that closely tracks measured kinematics. Although a static optimization criterion is used, the full state equations representing the activation and contraction dynamics [22] are incorporated into the forward dynamic simulation, and this approach has been validated for walking [10, 24]. Furthermore, the experimentally measured EMG profiles match closely the simulated muscle activation patterns without forced constraints. Therefore, in the authors' opinion, these musculoskeletal modeling limitations do not invalidate the results of the current investigation.

Despite the limitations discussed above, this study provides a foundation for future research using pathological and aging populations. The walking task presents limited risk and the relatively small changes in speed would be appropriate for most populations. Analysis using pathological and aging populations could illuminate changes in hip joint loading across speeds and in comparison to healthy populations. Identification of specific areas within the gait cycle where force discrepancies may occur (e.g., weight acceptance, propulsive, and toe off) could help focus management of care. In addition, analysis of other commonly used rehabilitation exercises could help identify activities with potentially hazardous joint loading and improve patient outcomes.

Competing Interests

There is no conflict of interests to declare.

Acknowledgments

This work was supported by an International Society of Biomechanics dissertation grant.

References

- [1] A. Vainionpää, R. Korpelainen, H. Sievänen, E. Vihriälä, J. Leppäluoto, and T. Jämsä, "Effect of impact exercise and its intensity on bone geometry at weight-bearing tibia and femur," *Bone*, vol. 40, no. 3, pp. 604–611, 2007.
- [2] D. T. Felson, "Osteoarthritis as a disease of mechanics," *Osteoarthritis and Cartilage*, vol. 21, no. 1, pp. 10–15, 2013.
- [3] G. Bergmann, G. Deuretzbacher, M. Heller et al., "Hip contact forces and gait patterns from routine activities," *Journal of Biomechanics*, vol. 34, no. 7, pp. 859–871, 2001.
- [4] M. O. Heller, G. Bergmann, G. Deuretzbacher et al., "Musculoskeletal loading conditions at the hip during walking and stair climbing," *Journal of Biomechanics*, vol. 34, no. 7, pp. 883–893, 2001.
- [5] M. G. Pandy, "Computer modeling and simulation of human movement," *Annual Review of Biomedical Engineering*, vol. 3, no. 1, pp. 245–273, 2001.

- [6] M.-J. Chung and M.-J. J. Wang, "The change of gait parameters during walking at different percentage of preferred walking speed for healthy adults aged 20–60 years," *Gait and Posture*, vol. 31, no. 1, pp. 131–135, 2010.
- [7] G. Giarmatzis, I. Jonkers, M. Wesseling, S. Van Rossom, and S. Verschueren, "Loading of hip measured by hip contact forces at different speeds of walking and running," *Journal of Bone and Mineral Research*, vol. 30, no. 8, pp. 1431–1440, 2015.
- [8] L. Modenese and A. T. M. Phillips, "Prediction of hip contact forces and muscle activations during walking at different speeds," *Multibody System Dynamics*, vol. 28, no. 1-2, pp. 157–168, 2012.
- [9] S. L. Delp, F. C. Anderson, A. S. Arnold et al., "OpenSim: open-source software to create and analyze dynamic simulations of movement," *IEEE Transactions on Biomedical Engineering*, vol. 54, no. 11, pp. 1940–1950, 2007.
- [10] D. G. Thelen and F. C. Anderson, "Using computed muscle control to generate forward dynamic simulations of human walking from experimental data," *Journal of Biomechanics*, vol. 39, no. 6, pp. 1107–1115, 2006.
- [11] A. R. De Asha, M. A. Robinson, and G. J. Barton, "A marker based kinematic method of identifying initial contact during gait suitable for use in real-time visual feedback applications," *Gait and Posture*, vol. 36, no. 3, pp. 650–652, 2012.
- [12] A. Rainoldi, G. Melchiorri, and I. Caruso, "A method for positioning electrodes during surface EMG recordings in lower limb muscles," *Journal of Neuroscience Methods*, vol. 134, no. 1, pp. 37–43, 2004.
- [13] J. T. Weinhandl, M. Joshi, and K. M. O'Connor, "Gender comparisons between unilateral and bilateral landings," *Journal of Applied Biomechanics*, vol. 26, no. 4, pp. 444–453, 2010.
- [14] J. T. Weinhandl and K. M. O'Connor, "Assessment of a greater trochanter-based method of locating the hip joint center," *Journal of Biomechanics*, vol. 43, no. 13, pp. 2633–2636, 2010.
- [15] E. S. Grood and W. J. Suntay, "A joint coordinate system for the clinical description of three-dimensional motions: application to the knee," *Journal of Biomechanical Engineering*, vol. 105, no. 2, pp. 136–144, 1983.
- [16] G. Wu, S. Siegler, P. Allard et al., "ISB recommendation on definitions of joint coordinate system of various joints for the reporting of human joint motion—part I: ankle, hip, and spine," *Journal of Biomechanics*, vol. 35, no. 4, pp. 543–548, 2002.
- [17] C. W. Spoor and F. E. Veldpaus, "Rigid body motion calculated from spatial co-ordinates of markers," *Journal of Biomechanics*, vol. 13, no. 4, pp. 391–393, 1980.
- [18] T.-W. Lu and J. J. O'Connor, "Bone position estimation from skin marker co-ordinates using global optimisation with joint constraints," *Journal of Biomechanics*, vol. 32, no. 2, pp. 129–134, 1999.
- [19] S. L. Delp, J. P. Loan, M. G. Hoy, F. E. Zajac, E. L. Topp, and J. M. Rosen, "An interactive graphics-based model of the lower extremity to study orthopaedic surgical procedures," *IEEE Transactions on Biomedical Engineering*, vol. 37, no. 8, pp. 757–767, 1990.
- [20] F. C. Anderson and M. G. Pandy, "Dynamic optimization of human walking," *Journal of Biomechanical Engineering*, vol. 123, no. 5, pp. 381–390, 2001.
- [21] G. T. Yamaguchi and F. E. Zajac, "A planar model of the knee joint to characterize the knee extensor mechanism," *Journal of Biomechanics*, vol. 22, no. 1, pp. 1–10, 1989.
- [22] F. E. Zajac, "Muscle and tendon: properties, models, scaling, and application to biomechanics and motor control," *Critical Reviews in Biomedical Engineering*, vol. 17, no. 4, pp. 359–411, 1989.
- [23] J. T. Weinhandl, J. E. Earl-Boehm, K. T. Ebersole, W. E. Huddleston, B. S. R. Armstrong, and K. M. O'Connor, "Anticipatory effects on anterior cruciate ligament loading during sidestep cutting," *Clinical Biomechanics*, vol. 28, no. 6, pp. 655–663, 2013.
- [24] K. M. Steele, M. S. DeMers, M. H. Schwartz, and S. L. Delp, "Compressive tibiofemoral force during crouch gait," *Gait and Posture*, vol. 35, no. 4, pp. 556–560, 2012.
- [25] J. L. Hicks, T. K. Uchida, A. Seth, A. Rajagopal, and S. L. Delp, "Is my model good enough? Best practices for verification and validation of musculoskeletal models and simulations of movement," *Journal of Biomechanical Engineering*, vol. 137, no. 2, Article ID 020905, 2015.
- [26] R. D. Crowninshield, R. C. Johnston, J. G. Andrews, and R. A. Brand, "A biomechanical investigation of the human hip," *Journal of Biomechanics*, vol. 11, no. 1-2, pp. 75–85, 1978.
- [27] H. Röhrle, R. Scholten, C. Sigolotto, W. Sollbach, and H. Kellner, "Joint forces in the human pelvis-leg skeleton during walking," *Journal of Biomechanics*, vol. 17, no. 6, pp. 409–424, 1984.
- [28] D. D. Larish, P. E. Martin, and M. Mungiole, "Characteristic patterns of gait in the healthy old," *Annals of the New York Academy of Sciences*, vol. 515, no. 1, pp. 18–32, 1988.
- [29] J. L. McCrory, S. C. White, and R. M. Lifeso, "Vertical ground reaction forces: objective measures of gait following hip arthroplasty," *Gait and Posture*, vol. 14, no. 2, pp. 104–109, 2001.
- [30] G. Lenaerts, F. De Groote, B. Demeulenaere et al., "Subject-specific hip geometry affects predicted hip joint contact forces during gait," *Journal of Biomechanics*, vol. 41, no. 6, pp. 1243–1252, 2008.
- [31] M. O. Heller, G. Bergmann, G. Deuretzbacher, L. Claes, N. P. Haas, and G. N. Duda, "Influence of femoral anteversion on proximal femoral loading: measurement and simulation in four patients," *Clinical Biomechanics*, vol. 16, no. 8, pp. 644–649, 2001.
- [32] R. D. Crowninshield and R. A. Brand, "A physiologically based criterion of muscle force prediction in locomotion," *Journal of Biomechanics*, vol. 14, no. 11, pp. 793–801, 1981.